Magnetotransport and the Shubnikov-de Haas effect in quasi-two-dimensional purple bronze $TlMo_6O_{17}$

2001 J. Phys.: Condens. Matter 13 311

(http://iopscience.iop.org/0953-8984/13/2/308)

INSTITUTE OF PHYSICS PUBLISHING JOURNAL OF PHYSICS: CONDENSED MATTER

J. Phys.: Condens. Matter **13** (2001) 311–318 www.iop.org/Journals/cm PII: S0953-8984(01)12636-6

Magnetotransport and the Shubnikov–de Haas effect in quasi-two-dimensional purple bronze $TlMo_6O_{17}$

Mingliang Tian[1], Song Yue[1], Jing Shi[2], Shiyan Li[1] and Yuheng Zhang[1]

[1] Structure Research Laboratory, University of Science and Technology of China, Hefei, 230026, Anhui, People's Republic of China
[2] Department of Physics, Wuhan University, Wuhan, 430072, People's Republic of China

Received 15 March 2000, in final form 29 November 2000

Abstract

Magnetotransport properties of quasi-two-dimensional thallium purple bronze were measured at different magnetic fields for $\boldsymbol{H} \parallel \boldsymbol{c}$. Huge positive magnetoresistance below the Peierls transition T_P and Shubnikov–de Haas oscillation in the high-field range were found. In the charge-density-wave (CDW) state below T_P, nonlinearity of the voltage–current characteristics due to the depinning of a CDW was also observed at 2 K and 14 T. These results supported the suggestion that the CDW gap opening below T_P still leaves small electron and/or hole pockets, but an applied magnetic field can remove these pockets to a great extent, thus leading to an enhanced gap.

1. Introduction

Molybdenum purple bronzes AMo_6O_{17} (A = Na, K and Tl) are quasi-two-dimensional (Q2D) metals at room temperature and undergo Peierls transitions at low temperatures accompanied by the formation of charge-density waves (CDW) [1–3]. Their structures can be described in terms of infinite slabs each consisting of four layers of ReO_3-like MoO_6 octahedra sharing corners, each of which is terminated on either side by a layer of MoO_4 tetrahedra sharing corners with adjacent MoO_6 octahedra in the same layer. These slabs are perpendicular to the c-direction and each is separated from its neighbour by a layer of monovalent metallic ions (Na^+, K^+ or Tl^+). The MoO_4 tetrahedra in adjacent layers do not share corners, so the Mo–O–Mo bonding, which is infinite in the ab-plane, is disrupted in the c-direction [4–6].

One notes that the mechanism of Peierls instability in Q2D metals is not straightforward due to the quasi-cylindrical Fermi surface (FS) with respect to an axis perpendicular to the 2D plane. The nesting of the FS is directly related to the so-called 'hidden' nesting, in which the FS can be viewed as a combination of quasi-one-dimensional (Q1D) structures with distinct 1D nesting vectors parallel to the 2D plane [7]. Normally, the FS does not show perfect nesting for real Q2D materials; the Peierls transition just removes parts of these Q1D FS, thus leaving some small electron and/or hole pockets in the avoided-crossing regions and inducing a metal–metal transition. Such a pseudo-1D FS model has been used to account for the physical properties of purple bronzes [3, 8] and monophosphate tungsten bronzes $(PO_2)_4(WO_3)_{2m}$

0953-8984/01/020311+08$30.00

[9–11]. However, evidence for nonlinear transport involving CDW sliding is still lacking for Q2D purple bronzes. This is because purple bronze behaves as a metal at zero magnetic field below T_P; it is very difficult to apply an electric field of the order of $E_T \sim 100$ mV cm^{-1}, which is what is required to depin the CDW.

Unusual huge positive magnetoresistances (MR) have been previously reported to arise in potassium purple bronze KMo_6O_{17} [1, 2] and the monophosphate tungsten bronzes $(PO_2)_4(WO_3)_{2m}$ ($m = 4$ and 6) [12, 13] below T_P, but few data are available for thallium purple bronze. In this paper, we describe detailed MR measurements on Q2D thallium purple bronze in the temperature range of 2–300 K. It is known that thallium purple bronze is perfectly stoichiometric with an ideal formula of $TlMo_6O_{17}$; in contrast, potassium purple bronze usually has a small amount of nonstoichiometry in K (traditionally, potassium purple bronze is written as $K_{0.9}Mo_6O_{17}$). Therefore, the nesting of the FS in thallium purple bronze is expected to be much better than that in the isostructural K purple bronze. The nonlinear response of CDW sliding might easily be observed at higher magnetic field due to the huge positive MR at low temperatures. Our magnetotransport studies on $TlMo_6O_{17}$ unambiguously confirmed the above speculations. The external cross-sectional area A_f of the FS perpendicular to the field in the thallium purple bronze is estimated to be about 6.7×10^{-4} Å^{-2}, which is smaller than that in KMo_6O_{17} with $A_f \sim 10^{-3}$ Å^{-2}. The threshold electric field, E_T, of the CDW depinning at 2 K and 14 T is about 81 mV cm^{-1}.

2. Experimental procedure

Single crystals of the thallium purple bronzes were grown by electrolytic reduction of a Tl_2CO_3–MoO_3 melt with an appropriate mole ratio. Platelet purple crystals with average dimensions of $4 \times 2 \times 0.5$ mm^3 were obtained on the cathode. The crystals were characterized by the x-ray diffraction technique. The temperature dependence of the MR was measured using the standard four-probe configuration in an Oxford ^{4}He cryostat with a superconducting magnet system providing magnetic fields up to 14 T. Freshly cleaved, thin single crystal was used for the measurements of the resistivity and V–I characteristics. The contacts were made by evaporating gold pads on the surface; gold wires 70 μm in diameter were anchored to the gold pads with silver paste. The distance between the two voltage contacts is about 1.0 mm. Direct current was supplied by a Keithley 220 current source, and the voltage was measured by a Keithley 182 nanovoltmeter. The temperature was controlled by a LakeShore 340 temperature controller. The whole system was controlled automatically by a computer.

3. Results

Figure 1 shows the in-plane resistance as a function of temperature for several magnetic fields parallel to c-axis (i.e., perpendicular to the ab-plane). The inset shows the plot with both scales logarithmic, to show clearly the low-temperature range. It is seen that the resistance at zero magnetic field exhibits an anomaly near about 110 K and a big hump near 80 K. This curve is in good agreement with previous reports [14, 15]. The anomaly at $T_P = 110$ K was attributed to the Peierls transition driven by the CDW instability, and the big hump results from the partial gradual removal of the FS, due to the Peierls gap opening. At lower temperature $T_M \sim 16$ K, a small minimum was clearly seen, below which the curve shows a slight upturn. For the magnetic field $\boldsymbol{H} \parallel \boldsymbol{c}$, the huge-positive-MR behaviour was only observed below the Peierls transition temperature T_P, and the resistance induced by the magnetic field increases much more quickly below T_M. The temperature T_M at the second anomaly moves to higher

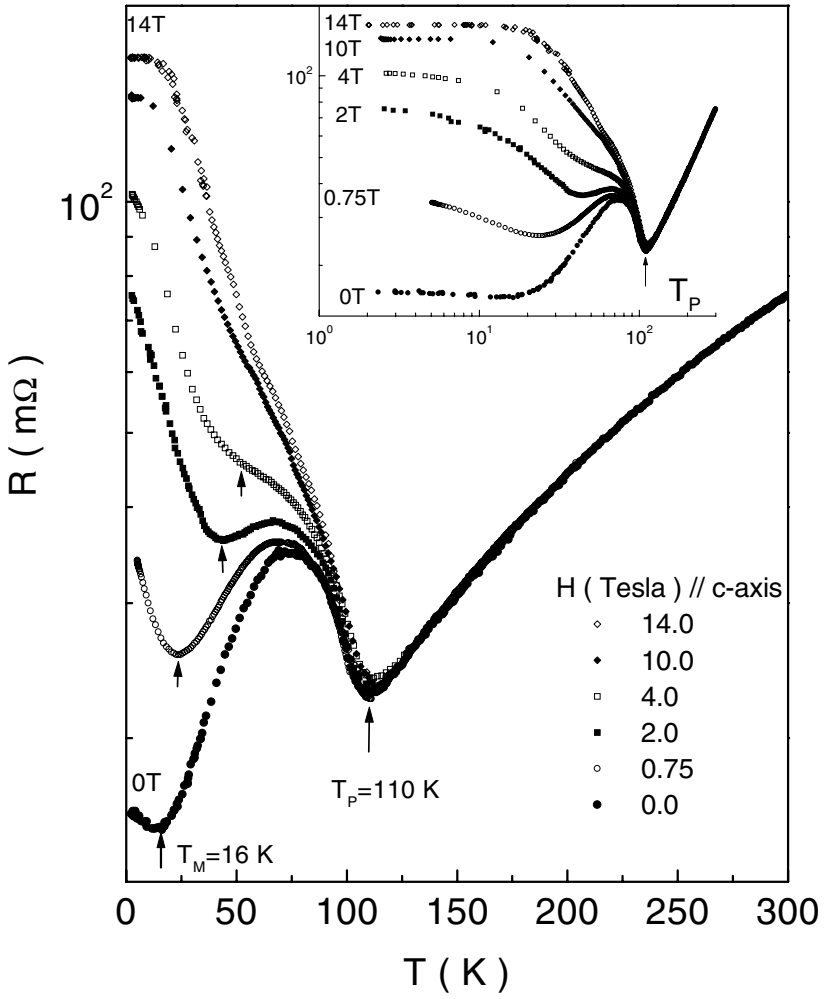

Figure 1. The temperature dependence of the resistance at various magnetic fields parallel to the c-axis; the inset shows the plot on logarithmic scales.

temperatures with increasing applied field, but the Peierls transition temperature T_P does not present a noticeable magnetic field effect in the range studied. At higher field $H \geqslant 10$ T, the resistance becomes almost temperature independent below about 16 K, and the second anomaly is suppressed by the magnetic field.

Figure 2 shows the in-plane MR $\Delta\rho(H)/\rho(0)$ at 2 K as a function of magnetic field for $\boldsymbol{H} \parallel \boldsymbol{c}$. The positive MR increases significantly with increasing magnetic field, and reaches about the order of $\Delta\rho(H)/\rho(0) \sim 930\%$ at 14 T. Two broad humps at 3.9 T and 8.8 T were clearly observed in the measured magnetic field range. The amplitude of the oscillatory part of the MR as a function of the magnetic field can be seen in the inset of figure 2 with the smooth background, indicated by the dashed line, subtracted.

Figure 3 shows the voltage–current (V–I) characteristics at 2 K and 14 T, at which the ohmic resistance of the sample reaches about 155 mΩ, which is 9.6 times larger than that at 2 K and zero magnetic field. When the voltage exceeds a critical voltage $V_T = 8.1$ mV, the V–I

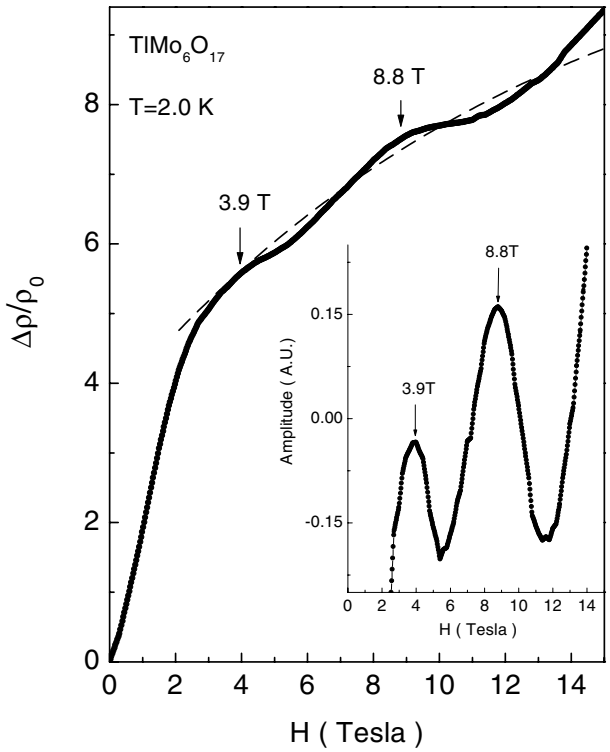

Figure 2. $\Delta\rho(H)/\rho_0$ at 2 K versus magnetic field; the inset shows the amplitude of the quantum oscillations with the smooth background, indicated by the dashed line, subtracted, versus the magnetic field.

curve deviates from a linear behaviour. The value of $V_T = 8.1$ mV corresponds to a threshold electrical field $E_T = V_T/d \sim 81$ mV cm^{-1}, which compares well with those in Q1D CDW systems like $NbSe_3$ ($E_T \sim 75$ mV cm^{-1}) [16–18] and $K_{0.3}MoO_3$ ($E_T \sim$ 50–500 mV cm^{-1}) [1, 2, 17, 18].

The huge-positive-MR results mentioned above were reproducible for all thallium purple bronzes investigated. Some details—for example, the amplitude of the oscillations and the tiny zero-field anomaly near T_M—usually exhibited some differences from sample to sample, but the main feature of the MR effect did not change too much. The sample on which measurements were made in this work is one showing strong oscillations in the MR curves.

4. Discussion

As shown in figure 2, the MR curve exhibits dramatic oscillation behaviour in the field range studied. If the observed wobbles result from the Shubnikov–de Haas effect, then the oscillation obeys the formula $H_n^{-1} = (2e/\hbar)(\pi/A_f)(n+\gamma)$, where γ is a constant, and H_n and A_f are, respectively, the magnetic field at the peak position of the oscillations and the extremal cross-sectional area of the FS perpendicular to the field $\boldsymbol{H}$ [3]. Since $H_{n+1}^{-1} - H_n^{-1} = 2e\pi/(\hbar A_f)$ and the period of H^{-1} is about 0.14 T^{-1} as evaluated from the two oscillations, we get $A_f \sim 6.7 \times 10^{-4}$ Å^{-2}. This value corresponds to an area of roughly 0.06% of the 2D Brillouin zone in the high-temperature state (the area of the 2D Brillouin zone at room temperature is

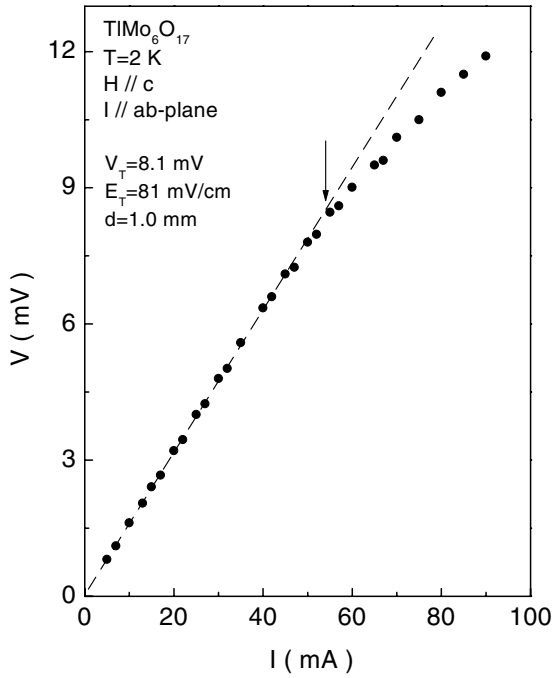

Figure 3. Voltage–current (V–I) characteristics at 2 K and 14 T; the nonlinear behaviour is seen above $E_T = 81$ mV cm^{-1}

about 1.1 as estimated from the unit-cell parameter). This result supported the suggestion that the Peierls transition just removes a part of the FS; some small electron and/or hole pockets still remain below T_P. Since the value of A_f for the thallium purple bronze is smaller than $A_f \sim 10^{-3}$ Å^{-2} for the potassium purple bronze obtained from MR measurement [1, 2], the nesting of the FS in the Tl purple bronze would be much better than that in the K purple bronze.

The temperature dependence of the huge positive MR effect observed in the thallium purple bronze is very similar to that in the potassium purple bronze [1, 2]. This indicated that the two compounds should have very similar electronic structures. Figure 4 shows the MR as a function of H^2; the curve deviates considerably from linearity in the range studied. The inset shows $\Delta\rho(H)/\rho(0)$ versus H on scales that are both logarithmic; we get a power-law relation $\Delta\rho(H)/\rho(0) = AH^\alpha$ with $\alpha = 1.26$ in the low-field range of 0–2 T. These results indicated that the normal semiclassical formula $\Delta\rho(H)/\rho(0) = \mu H^2$ for a metal is not suitable for describing the field dependence of the MR effect. Since the huge positive MR effect was only observed below the Peierls transition temperature T_P, the nature of the MR effect must be closely related to the variations of the FS structures induced by the magnetic field in the CDW state.

Previously, Balseiro and Falicov (BF) [19] developed a theoretical model for strongly anisotropic metals in a magnetic field; they predicted that a high magnetic field parallel to the FS can considerably modify a FS with an imperfect nesting. The small pieces of electron and hole pockets left below T_P can be destroyed progressively by the applied magnetic field, which results in a better effective nesting and an enhanced gap. This model was usually used to explain the positive MR effect in Q1D $NbSe_3$ [16, 20, 21]. Since the FS structures in the Q2D purple bronzes can be considered as combinations of several 'hidden' Q1D structures, the BF

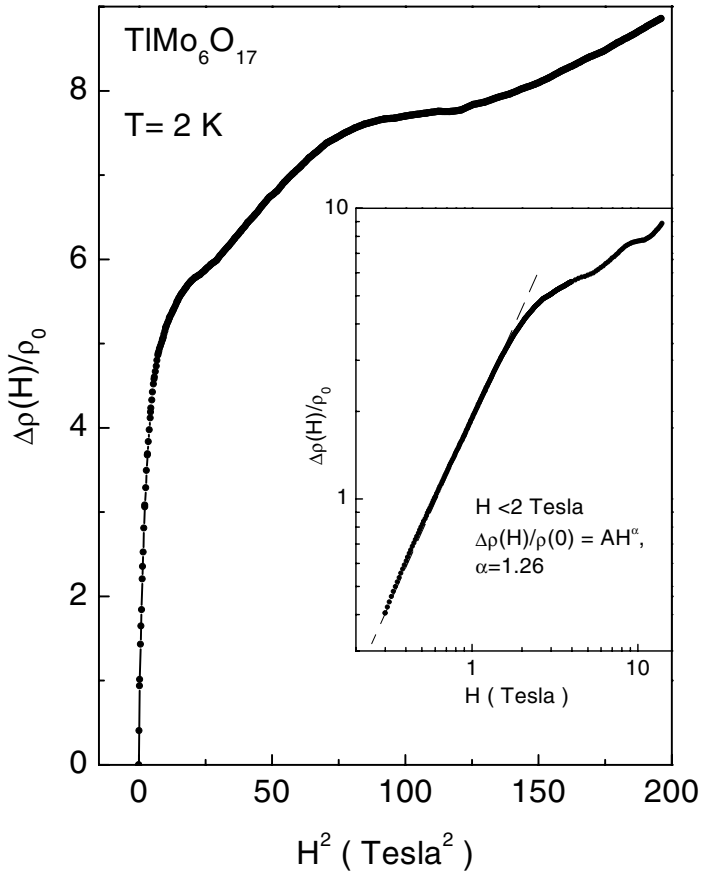

Figure 4. $\Delta\rho(H)/\rho_0$ versus H^2 at 2 K; the inset shows $\Delta\rho(H)/\rho_0$ versus H on logarithmic scales, showing $\Delta\rho(H)/\rho_0 \propto H^{\alpha}$ with $\alpha = 1.26$.

theory seems also to be suitable to account for our MR data on purple bronze, qualitatively. The core of the BF model concerns an enhanced gap and a considerable reduction in the number of normal carriers induced by the applied field below T_P; some evidence has been provided by Parilla *et al* [22] on the basis of measurements of the narrow-band noise as a function of magnetic field in Q1D $NbSe_3$—but this was also contradicted subsequently by Tritt *et al* [23] and Lin *et al* [24]. Therefore, the nature of the huge positive MR effect in Q2D purple bronze is still an open question in theory.

In figure 3, nonlinear voltage–current (V–I) characteristics at 2 K and 14 T are clearly seen, for the first time. In order to exclude a possible Joule-heating effect, we anchored the sample on a sapphire substrate, then soldered the substrate on a large copper holder. Rectangular direct current with a duration of about 200 ms was supplied by controlling the Keithley 220 current source via a computer; the interval between two pulses is 10 s. We detected a 1.5 K rise of the temperature at $I = 90$ mA during an interval of 200 ms. From figure 1, it was noted that the resistance at 14 T is insensitive to the temperature below about 16 K; it almost keeps to a constant value of 155 mΩ. Therefore, the remarkable deviation of the V–I characteristics from linearity above $E_T = 81$ mV cm^{-1} does not result from the heating effect; it can be attributed to the sliding of the CDW condensate depinned from the impurities. The observation of non-

linear V–I characteristics at 14 T and 2 K supports the idea of a field-induced enhanced gap. The threshold electric field obtained, 81 mV cm^{-1}, is also comparable with those for $NbSe_3$ and blue bronzes.

The second anomaly of the resistance at T_M, which was enhanced by the applied magnetic field, can be attributed to the second Peierls instability. Bjelis and Maki [25] and Zanchi *et al* [26] have carefully studied the influence of the magnetic field on the collective properties of the density waves (CDW or SDW) with an imperfectly nesting FS. They predicted that, in the case of strong orbital coupling with the magnetic field, the critical temperature T_P of a CDW or SDW state will increase with increasing magnetic field at moderate fields; if one considers the contribution of the Pauli effect, T_c will decrease greatly with the increase of the field. Therefore, the increase of the second anomalous temperature, T_M with the increase of the applied magnetic field might be associated with the effect of strong orbital coupling.

In summary, the MR properties of Q2D thallium purple bronzes have been studied between 2 and 300 K. It is concluded that:

(i) the second anomaly near about 16 K is associated with the second Peierls instability;
(ii) the Peierls transition at T_P just removes a part of the FS; some small electron and/or hole pockets still remain below T_P;
(iii) the positive MR effect can be qualitatively explained by the BF model, where the applied field can improve the nesting of the FS and thus lead to an enhanced gap;
(iv) the nonlinear V–I characteristics observed at 2 K and 14 T provide evidence of sliding of the CDW depinned from the pinning centres.

Acknowledgments

The authors would like to thank Mr Qiang Cao for technical help in the experiment. This work was supported by the Natural Science Foundation of China.

References

[1] Schlenker C, Dumas J, Escribe-Filippini C, Guyot H, Marcus J and Fourcaudot G 1985 *Phil. Mag.* B **52** 643
[2] Dumas J and Schlenker C 1993 *Int. J. Mod. Phys.* B **7** 4050
[3] Schlenker C 1996 *Physics and Chemistry of Low-Dimensional Inorganic Conductors (NATO ASI Series B: Physics, vol 354* ed C Schlenker, J Dumas, M Greenblatt and S van Smaalen (New York: Plenum) p 115
[4] Vincent H, Ghedira M, Marcus J, Mercier J and Schlenker C 1983 *J. Solid State Chem.* **47** 113
[5] Onada M, Matsuda Y and Sato M 1987 *J. Solid State Chem.* **69** 67
[6] Ganne M, Dion M, Boumaza A and Tournoux M 1986 *Solid State Commun.* **59** 137
[7] Whangbo M H, Canadell E, Foury P and Pouget J P 1991 *Science* **252** 96
[8] Pouget J P 1989 *Low Dimensional Properties of Molybdenum Bronzes and Oxides* ed C Schlenker (Dordrecht: Kluwer Academic) p 87
[9] Canadell E and Whangbo M H 1991 *Chem. Rev.* **91** 965
Canadell E and Whangbo M H 1991 *Phys. Rev.* B **43** 1894
[10] Wang E, Greenblatt M, Rachidi I E, Canadell E, Whangbo M H and Vadlamannati S 1989 *Phys. Rev.* B **39** 12 969
[11] Teweldemedhin Z S, Ramanujachary K V and Greenblatt M 1992 *Phys. Rev.* B **46** 7897
[12] Schlenker C, Hess C, Le Touze C and Dumas J 1996 *J. Physique* I **6** 2061
[13] Hess C, Schlenker C, Dumas J, Greenblatt M and Teweldemedhin Z S 1996 *Phys. Rev.* B **54** 4581
[14] Tian M, Chen L, Sekine H, Shi J, Wang R P, Mao Z Q and Zhang Y H 1997 *Phys. Lett.* A **234** 477
[15] Ramanujachary K V, Collins B T, Greenblatt M and Waszczak J V 1986 *Solid State Commun.* **59** 647
[16] Coleman R V, Eiserman G, Everson M P, Johnson A and Falicov L M 1985 *Phys. Rev. Lett.* **55** 863
Coleman R V, Eiserman G, Everson M P, Johnson A and Falicov L M 1990 *Phys. Rev.* B **41** 460
[17] Gruner G 1988 *Rev. Mod. Phys.* **60** 1129
[18] Zettl A and Gruner G 1985 *Phys. Rep.* **119** 117
[19] Balseiro C A and Falicov L M 1985 *Phys. Rev. Lett.* **55** 2336

Balseiro C A and Falicov L M 1986 *Phys. Rev.* B **34** 863
[20] Monceau P and Briggs A 1978 *J. Phys. C: Solid State Phys.* **11** L465
[21] Everson M P, Eiserman G, Johnson A and Coleman R V 1984 *Phys. Rev. Lett.* **52** 1721
Everson M P, Eiserman G, Johnson A and Coleman R V 1984 *Phys. Rev.* B **30** 3582
[22] Parilla P, Hundley M F and Zettl A 1986 *Phys. Rev. Lett.* **57** 619
Hundley M F, Parilla P and Zettl A 1986 *Phys. Rev.* B **34** 5970
Hundley M F, Parilla P and Zettl A 1987 *Solid State Commun.* **61** 587
[23] Tritt T M, Ehrlich A C, Gillespie D J and Tessema G X 1991 *Phys. Rev.* B **43** 7254
Tritt T M, Ehrlich A C, Gillespie D J and Tessema G X 1988 *Phys. Rev. Lett.* **61** 1776
[24] Lin T M, Duan H M and Zhang D L 1988 *Europhys. Lett.* **5** 169
[25] Bjelis A and Maki K 1990 *Phys. Rev.* B **42** 10 275
Bjelis A and Maki K 1999 *J. Physique* IV **9** 203
[26] Zanchi D, Bjelis A and Montambaux G 1996 *Phys. Rev.* B **53** 1240